Exploiting Vibrational Strong Coupling to Make an Optical Parametric Oscillator Out of a Raman Laser

Javier del Pino,[1] Francisco J. Garcia-Vidal,[1,2,*] and Johannes Feist[1,†]
[1]Departamento de Física Teórica de la Materia Condensada and Condensed Matter Physics Center (IFIMAC), Universidad Autónoma de Madrid, E-28049 Madrid, Spain
[2]Donostia International Physics Center (DIPC), E-20018 Donostia/San Sebastián, Spain
(Received 15 July 2016; revised manuscript received 14 October 2016; published 29 December 2016)

When the collective coupling of the rovibrational states in organic molecules and confined electromagnetic modes is sufficiently strong, the system enters into vibrational strong coupling, leading to the formation of hybrid light-matter quasiparticles. In this Letter, we demonstrate theoretically how this hybridization in combination with stimulated Raman scattering can be utilized to widen the capabilities of Raman laser devices. We explore the conditions under which the lasing threshold can be diminished and the system can be transformed into an optical parametric oscillator. Finally, we show how the dramatic reduction of the many final molecular states into two collective excitations can be used to create an all-optical switch with output in the midinfrared.

DOI: 10.1103/PhysRevLett.117.277401

When the coherent interaction between a confined light mode and vibrational matter excitations becomes faster than the relevant decoherence processes, the system can enter into vibrational strong coupling (VSC) [1–6]. The fundamental excitations of the two systems then become inextricably linked and can be described as hybrid light-matter quasiparticles, so-called vibropolaritons, that combine the properties of both ingredients. In particular, the use of vibrational modes that are both IR and Raman active allows us to probe vibropolaritons through Raman scattering mediated by their material component [7–9].

On the other hand, while the cross sections for Raman scattering are typically small, the process can become highly efficient under strong driving if the scattered Stokes photons accumulate sufficiently to lead to stimulated Raman scattering [10]. The effective energy conversion from input to output beam can then be exploited to fabricate a highly tunable Raman laser. Raman lasers have been realized using a variety of nonlinear media and configurations, such as under pulsed operation in optical fibers [11], nonlinear crystals [12], gases [13], or silicon [14], as well as under continuous-wave operation in silicon [15,16], silica [17], and molecular hydrogen [18]. Since the threshold powers for these systems are typically large, they suffer from detrimental effects such as Kerr nonlinearities, four-wave mixing, and heat deposition [12].

In this Letter, we propose and theoretically demonstrate that the hybrid light-matter nature of vibropolaritons can be exploited to obtain photon emission from the vibrationally excited final states of a Raman laser. A single-output Raman laser device then becomes analogous to a nondegenerate optical parametric oscillator (OPO), which converts an input pump beam into two coherent output beams at different frequencies [19]. In the present case, sketched in Fig. 1, the "signal" beam in the visible spectrum corresponds to the conventional Raman laser output, while the "idler" beam is emitted by the vibropolaritons in the mid-IR. Importantly, the signal and idler beams emitted by OPOs are coherent and have a stable phase relation, as well as providing possibly entangled pairs of photons with

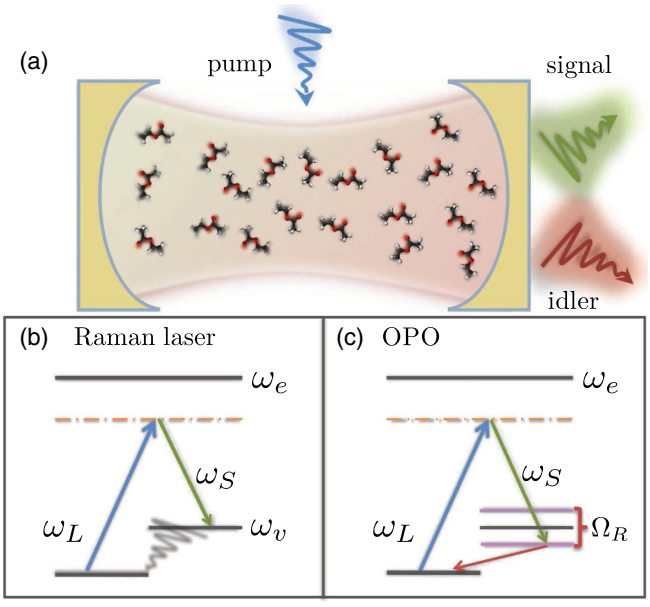

FIG. 1. (a) Sketch of the setup to convert a Raman laser into an OPO through vibrational strong coupling. (b) In a Raman laser, Raman scattering of the pump (blue arrows) leads to vibrationally excited final states that decay nonradiatively, so that only a signal beam (green) is emitted. (c) Under strong coupling of the vibrational excitations with a resonant cavity mode, the new final states (vibropolaritons) can decay through photon emission, producing an idler beam as a second output.

nonclassical correlations [20–25]. A compact solid-state OPO as proposed here could thus have applications in quantum information transmission and storage [26,27]. In addition to the OPO properties, our approach has the advantage over Raman lasers of effectively getting rid of the energy deposited into material vibrations; instead of being dissipated as heat, this energy is emitted in the form of photons. Finally, we show that the coexistence of the upper and lower polariton modes with very similar properties can be exploited to produce an all-optical switch [28,29]. Here, one (gate) pump beam can be used to switch Raman lasing of a second (signal) pump beam.

The system we consider [sketched in Fig. 1(a)] consists of a material with a vibrational transition that is both IR and Raman active, placed inside a resonator (e.g., a microcavity). The resonator supports at least two confined modes: a mid-IR mode used to achieve VSC with the vibrational transition and an optical mode used to accumulate the scattered Stokes photons. We model the material as a set of N noninteracting three-level quantum emitters, formed by the ground state $|g\rangle$ (energy $\omega_g \equiv 0$), the first excited vibrational mode $|v\rangle$ (energy ω_v), and an electronically excited state $|e\rangle$ (energy ω_e) [8]. While this model can naturally represent organic molecules (as used in current experiments achieving VSC), we note that it can also be used to treat systems such as the nonlinear crystals utilized in existing Raman lasers. Under off-resonant driving, as will be considered here, the parameters of $|e\rangle$ can be adjusted such that it represents the full rovibrational manifold of electronically excited states.

The system Hamiltonian is given by $\hat{H}_s = \hat{H}_v + \hat{H}_o$, where $\hat{H}_v$ describes the vibrational excitations and their coupling to the mid-IR cavity mode, and $\hat{H}_o$ describes the excitations and cavity mode at optical energies. We use the rotating wave approximation (RWA), which removes off-resonant couplings, under the assumption that the two frequency regions (mid-IR and optical) are well separated. The vibrational Hamiltonian $\hat{H}_v$ is then given by (setting $\hbar = 1$ here and in the following)

$$\hat{H}_v = \omega_c \hat{a}_c^\dagger \hat{a}_c + \sum_{i=1}^{N} [\omega_v \hat{\sigma}_{vv}^{(i)} + (g \hat{a}_c^\dagger \hat{\sigma}_{gv}^{(i)} + \text{H.c.})], \quad (1)$$

where ω_c is the frequency of the mid-IR cavity mode with annihilation operator $\hat{a}_c$, while $\hat{\sigma}_{ab} = |a\rangle\langle b|$ denotes the transition operator between states $|b\rangle$ and $|a\rangle$, with superscripts specifying the molecule that the operator applies to. The light-matter interaction strength is measured by g, which depends on the single-photon electric field strength of the mid-IR cavity mode and the change of the molecular dipole moment under displacement from the equilibrium position.

Assuming zero detuning ($\omega_c = \omega_v$) for simplicity, the eigenstates of $\hat{H}_v$ are formed by (i) two vibropolaritons, $|\pm\rangle = (1/\sqrt{2})(\hat{a}_c^\dagger|G\rangle \pm |B\rangle)$, symmetric and antisymmetric hybridizations of the cavity mode with the collective bright state of the molecular vibrations, $|B\rangle = (1/\sqrt{N}) \sum_{i=1}^{N} |v^{(i)}\rangle$. Here, $|G\rangle$ denotes the global ground state. The polaritons have eigenfrequencies $\omega_\pm = \omega_v \pm g\sqrt{N}$, separated by the Rabi splitting $\Omega_R = 2g\sqrt{N}$. The other eigenstates are (ii) $N-1$ so-called dark states $|d\rangle$ orthogonal to $|B\rangle$ that have eigenfrequencies ω_v and no electromagnetic component.

We first treat the dynamics of the system under external driving of a single pump mode at frequency ω_L (not resonant with any cavity mode); see Fig. 1. The optical-frequency Hamiltonian $\hat{H}_o$ then contains the electronic excitations of the molecules, the pump field (which we quantize in order to be able to describe depletion [30]), the cavity mode in the optical (frequency ω_S), and the interactions between the molecular transitions and the optical modes, leading to

$$\hat{H}_o = \omega_S \hat{n}_S + \omega_L \hat{n}_L + \sum_{i=1}^{N} [\omega_e \hat{\sigma}_{ee}^{(i)} + (g_S \hat{a}_S \hat{\sigma}_{ve}^{(i)\dagger} + g_L \hat{a}_L \hat{\sigma}_{ge}^{(i)\dagger} + \text{H.c.})], \quad (2)$$

where $\hat{n}_L = \hat{a}_L^\dagger \hat{a}_L$ and $\hat{n}_S = \hat{a}_S^\dagger \hat{a}_S$ are the photon number operators for the pump laser and confined cavity mode, which are coupled (within the RWA) to the ground-excited and excited-vibrational transitions in the molecules with coupling strengths g_L and g_S, respectively.

When the driving laser is far-off-resonant to the electronic transition such that the hierarchy condition $\omega_e \gg \omega_L \gg \omega_v$ is satisfied, we can adiabatically eliminate the electronically excited states from the problem [31,32]. If the laser frequency is, moreover, chosen such that Raman scattering into the "Stokes" cavity mode S is resonant with one of the polariton modes, i.e., $\omega_L = \omega_S + \omega_p$ (with $p = +$ or $p = -$), scattering to the other polaritonic mode can be neglected under a second RWA. This gives the following effective system Hamiltonian (for details see the Supplemental Material [33]):

$$\hat{H}_{\text{eff}} \simeq \omega_L \hat{n}_L + \omega_S \hat{n}_S + \omega_p \hat{\sigma}_{pp} - g_{\text{eff}}^p (\hat{a}_L \hat{a}_S^\dagger \hat{\sigma}_{Gp}^\dagger + \text{H.c.}), \quad (3)$$

where the effective coupling occurs between laser photons and pairs of Stokes photons and polaritons, while the dark modes are not excited. The coupling strength is given by

$$g_{\text{eff}}^p = \sqrt{\frac{N}{2}} \frac{g_S g_L}{\omega_e - (\omega_p + \omega_S)}, \quad (4)$$

and is not sensitive to the Rabi splitting of the polaritons. This agrees with the case of linear Raman scattering, where theory predicts a redistribution of the scattering cross section of the system without further enhancement [8,9].

When deriving g^p_{eff}, we have assumed perfect spatial overlap between the three involved modes L, S, and p; inclusion of the spatial profile would lead to the renormalization $g^\eta_{\mathrm{eff}} \to g^\eta_{\mathrm{eff}}\mathcal{S}$, with $\mathcal{S}$ the overlap integral.

The trilinear interaction in the effective Hamiltonian Eq. (3) is analogous to a nondegenerate OPO, converting an input laser beam into two new modes, the "signal" (Stokes beam) and "idler" (vibropolaritons) [19]. For a standard Raman laser, this analogy is merely formal [10], since most of the excitation in the vibrationally excited states decays nonradiatively and no idler beam is emitted. In the VSC regime, however, the hybrid light-matter nature of the polaritons imbues them with a photonic component, leading to efficient outcoupling in the form of photons. This makes the analogy complete and provides an approach towards converting a Raman laser into an OPO, as sketched in Fig. 1(c). Such a setup could be realized in cavities made from dielectric materials with low losses both at optical and mid-IR frequencies, for example, based on distributed Bragg reflectors, which have previously been used to achieve strong coupling with both vibrational modes and excitons [6,38]. In the Supplemental Material, we show a concrete implementation of such a cavity based on silicon carbide-silicon dioxide mirrors, with PVAc as the active material [33].

We next discuss the role of losses and dephasing. Within the standard Lindblad master-equation formalism, the density operator $\hat{\rho}$ evolves according to

$$\partial_t\hat{\rho} = -i[\hat{H}_{\mathrm{eff}},\hat{\rho}] + \kappa_S\mathcal{L}_{\hat{a}_S}[\hat{\rho}] + \kappa_L\mathcal{L}_{\hat{a}_L}[\hat{\rho}] + \tilde{\Gamma}_{\mathrm{vib}}[\hat{\rho}], \quad (5)$$

where $\mathcal{L}_X[\hat{\rho}] = \hat{X}\hat{\rho}\hat{X}^\dagger - \frac{1}{2}\{\hat{X}^\dagger\hat{X},\hat{\rho}\}$. The loss rates of the Stokes and quantized laser modes due to leakage out of the cavity and absorption losses are given by κ_S and κ_L, respectively. The term $\tilde{\Gamma}_{\mathrm{vib}}$ summarizes all decoherence mechanisms affecting the vibrationally excited subspace. Under weak coupling, these consist of nonradiative decay of the vibrational excitations to the ground state ($\gamma_v\mathcal{L}_{\hat{\sigma}_{gv}}$) and pure dephasing induced by elastic collisions with background phonons ($\gamma_\varphi\mathcal{L}_{\hat{\sigma}_{vv}}$). In the VSC regime, the polaritons additionally decay through the losses associated with the mid-IR cavity (κ_c), but the influence of inhomogeneous broadening and dephasing can be suppressed for large enough Rabi splitting [4,39]. The effective decay of the polaritons ($\Gamma_\pm\mathcal{L}_{\hat{\sigma}_{g\pm}}$) can then have a rate as small as $\Gamma_\pm \approx (\kappa_c+\gamma_v)/2$, significantly below the average of the bare-molecule ($\gamma_v+\gamma_\varphi$) and mid-IR cavity (κ_c) linewidths. We note here that even under weak coupling, the vibrational excitations can be made to decay mostly through radiation under some circumstances. This regime is reached when the coupling to the cavity is faster than nonradiative decay processes, but not faster than the cavity lifetime, and thus only exists for "bad cavities," while high-quality cavities directly enter the strong coupling regime as the coupling is increased.

In order to characterize the threshold condition and quantum yield of the VSC-based OPO described above, we calculate the steady-state populations under continuous-wave driving of the pump mode, with

$$\hat{H}'_{\mathrm{eff}} = \hat{H}_{\mathrm{eff}} + \Phi_{\mathrm{in}}\sqrt{\kappa_L}(\hat{a}_L e^{-i\omega_L t} + \hat{a}_L^\dagger e^{i\omega_L t}), \quad (6)$$

where Φ_{in} parametrizes the driving strength. The results derived below are also valid under time-dependent driving as long as the pump amplitude Φ_{in} varies more slowly than the time required to reach the steady state. We solve the Lindblad master equation within the standard mean-field approximation, in which all fields are assumed to be described by coherent amplitudes [40]. This leads to semiclassical Heisenberg-Langevin equations of motion in terms of the slowly varying amplitudes $\alpha_L = \langle\hat{a}_L\rangle e^{i\omega_L t}$, $\alpha_S = \langle\hat{a}_S\rangle e^{i\omega_S t}$, and $\psi_p = \langle\hat{\sigma}_{Gp}\rangle e^{i\omega_p t}$, given by

$$\partial_t\alpha_L = ig^p_{\mathrm{eff}}\psi_p\alpha_S - \kappa_L\alpha_L + i\sqrt{\kappa_L}\Phi_{\mathrm{in}}, \quad (7a)$$

$$\partial_t\alpha_S = ig^p_{\mathrm{eff}}\psi_p^*\alpha_L - \kappa_S\alpha_S, \quad (7b)$$

$$\partial_t\psi_p = ig^p_{\mathrm{eff}}\alpha_S^*\alpha_L - \Gamma_p\psi_p. \quad (7c)$$

The corresponding steady-state solutions (which agree with the classical treatment of an OPO [41]) can be parametrized in terms of $f = \Phi_{\mathrm{in}}/\Phi_{\mathrm{th}}$, where $\Phi_{\mathrm{th}} = \sqrt{\kappa_L\kappa_S\Gamma_p}/g^p_{\mathrm{eff}}$ is the threshold value for the driving parameter. Below threshold ($f<1$), neither the polariton nor the Stokes mode are populated ($|\psi_p|^2 = |\alpha_S|^2 = 0$), while the pump mode has population $|\alpha_L|^2 = f^2\Phi^2_{\mathrm{th}}/\kappa_L$. Above threshold ($f \geq 1$), the pump amplitude becomes independent of the driving power (so-called pump clamping), $|\alpha_L|^2 = \Phi^2_{\mathrm{th}}/\kappa_L$, while the Stokes and polariton mode occupations grow linearly with input power, $|\psi_p|^2 = (f-1)\Phi^2_{\mathrm{th}}/\Gamma_p$ and $|\alpha_S|^2 = (f-1)\Phi^2_{\mathrm{th}}/\kappa_S$. This implies that the conversion efficiency approaches 100% if the pumping is sufficiently strong. Explicitly, the quantum yield for conversion of input photons to pairs of Stokes photons and polaritons follows the simple relation

$$\mathcal{Q} = \frac{P_S/\omega_S}{P_{\mathrm{in}}/\omega_L} = 1 - \frac{1}{f}, \quad (8)$$

where $P_S/\omega_S = \kappa_S|\alpha_S|^2$ ($= P_p/\omega_p$) is the flux of emitted Stokes photons, and $P_{\mathrm{in}} = \omega_L\Phi_{\mathrm{in}}\Phi_{\mathrm{th}}$ is the input power.

The number of photons emitted at the vibropolariton frequency (typically in the mid-IR [1]) is equal to the number of generated Stokes photons, multiplied by the radiative emission efficiency of the polaritons, $\beta = \Gamma^{\mathrm{rad}}_p/\Gamma_p$. For zero detuning and a mid-IR cavity without nonradiative losses (such as a dielectric cavity [6]), this is given by $\beta = \kappa_c/(\kappa_c+\gamma_v)$, which is close to unity for the experimentally relevant regime $\kappa_c \gg \gamma_v$. In a

standard Raman laser, the energy deposited into the vibrational modes is converted to heat, limiting the achievable powers [12,19]. In contrast, the vibropolariton Raman OPO proposed here converts this energy efficiently into an additional coherent output beam at mid-IR frequencies, and thus simultaneously reduces heating significantly.

Furthermore, the ratio between the thresholds for polariton-based OPO operation under strong coupling and for the bare-molecule Raman laser under weak coupling is given by

$$\frac{\Phi_{\mathrm{th}}^{\mathrm{SC}}}{\Phi_{\mathrm{th}}^{\mathrm{WC}}} = \sqrt{\frac{\Gamma_p}{\gamma_v + \gamma_\varphi}} \approx \sqrt{\frac{\kappa_c}{2\gamma_\varphi}}. \tag{9}$$

This demonstrates that for the common case that the inhomogeneous width and dephasing of the vibrational modes are faster than the cavity losses ($\gamma_\varphi > \kappa_c$), the vibropolariton Raman OPO has a lower threshold power than the equivalent Raman laser. In addition, depending on the relative lifetimes of the vibropolaritons Γ_p and the Stokes photons κ_S, there can be significant accumulation of population in the vibropolariton mode, suggesting a road map towards achieving vibropolariton condensation (in analogy to exciton-polariton condensation [42]) based on the high efficiency of stimulated Raman scattering.

We next show how the coexistence of two vibropolariton modes with similar properties allows us to turn the system into an all-optical switch where emission at one frequency is switched by input at another frequency [28,29]. This is achieved by including a second pump field, with the two pump frequencies chosen to make the Raman process to the two polariton modes $|+\rangle$ and $|-\rangle$ resonant with the same Stokes frequency,

$$\omega_{L\pm} = \omega_S + \omega_\pm. \tag{10}$$

Following the procedure of adiabatic elimination and again performing a second RWA to remove terms rotating at frequencies $\pm\Omega_R$ (see Ref. [33] for details), we obtain the new effective Hamiltonian,

$$\hat{H}_{\mathrm{eff}}^{(2)} \simeq \omega_S \hat{n}_S + \sum_{\eta=\{\pm\}} [\omega_{L\eta}\hat{n}_{L\eta} + \omega_\eta \hat{\sigma}_{\eta\eta} - g_{\mathrm{eff}}^{\eta}(\hat{\sigma}_{G\eta}\hat{a}_S\hat{a}_{L\eta}^{\dagger} + \mathrm{H.c.})], \tag{11}$$

with corresponding Heisenberg-Langevin equations in the mean-field approximation (and under driving):

$$\partial_t \alpha_{L\pm} = i g_{\mathrm{eff}}^{\pm} \psi_\pm \alpha_S - \kappa_L \alpha_{L\pm} + i\sqrt{\kappa_{L\pm}}\Phi_{\mathrm{in}}^{\pm}, \tag{12a}$$

$$\partial_t \alpha_S = i g_{\mathrm{eff}}^{+} \psi_+^* \alpha_{L+} + i g_{\mathrm{eff}}^{-} \psi_-^* \alpha_{L-} - \kappa_S \alpha_S, \tag{12b}$$

$$\partial_t \psi_\pm = i g_{\mathrm{eff}}^{\pm} \alpha_S^* \alpha_{L\pm} - \Gamma_\pm \psi_\pm. \tag{12c}$$

The basic idea for achieving all-optical switching is then to use one of the pump lasers as the input signal ($s = \pm$) and the other pump laser as a gate ($g = \mp$). If the gate beam is turned off, the system is identical to the OPO discussed up to now, and a weak signal beam ($f_s = \Phi_{\mathrm{in}}^s/\Phi_{\mathrm{th}}^s < 1$) will not lead to lasing, such that the corresponding polaritonic mode is not populated. On the other hand, if the gate beam is strong enough to support OPO operation ($f_g > 1$), the Raman scattering for even a weak signal beam is stimulated by the macroscopic population of the Stokes mode, $|\alpha_S|^2 \gg 1$. We next demonstrate this idea in more detail by solving for the steady state.

The relative phases of the different modes are fixed in the steady state, leading to five equations only involving the absolute amplitudes:

$$\kappa_S|\alpha_S| = \sum_{\eta=\{\pm\}} g_{\mathrm{eff}}^{\eta}|\psi_\eta||\alpha_{L\eta}|, \tag{13a}$$

$$\Gamma_\pm|\psi_\pm| = g_{\mathrm{eff}}^{\pm}|\alpha_{L\pm}||\alpha_S|, \tag{13b}$$

$$\kappa_{L\pm}|\alpha_{L\pm}| = \sqrt{\kappa_{L\pm}}\Phi_{\mathrm{in}}^{\pm} - g_{\mathrm{eff}}^{\pm}|\psi_\pm||\alpha_S|. \tag{13c}$$

These equations can be reduced to a quartic polynomial, which permits an analytical solution. The general case is treated in the Supplemental Material [33], while here we focus on the case that the two thresholds are identical, $\Phi_{\mathrm{th}}^{+} = \Phi_{\mathrm{th}}^{-} = \Phi_{\mathrm{th}}$, which allows for simple analytical expressions. In particular, the threshold condition can then be simplified to $f_{\mathrm{tot}} > 1$, where $f_{\mathrm{tot}} = \sqrt{f_+^2 + f_-^2}$. Below threshold ($f_{\mathrm{tot}} < 1$), the mean-field populations are identical to the single-pump case, with neither the polariton nor the Stokes modes being populated ($|\psi_\pm|^2 = |\alpha_S|^2 = 0$), while the pump mode populations are just determined by the driving of each mode, $|\alpha_{L\pm}|^2 = f_\pm^2\Phi_{\mathrm{th}}^2/\kappa_L$. Above threshold ($f_{\mathrm{tot}} \geq 1$), the Stokes and polariton mode occupations are given by $|\alpha_S|^2 = (f_{\mathrm{tot}} - 1)\Phi_{\mathrm{th}}^2/\kappa_S$ and $|\psi_\pm|^2 = (f_{\mathrm{tot}} - 1)\Phi_{\mathrm{th}}^2 f_\pm^2/(f_{\mathrm{tot}}^2\Gamma_\pm)$. In contrast to the single-mode OPO case, the pump mode populations are not clamped to a fixed value above threshold, but are given by $|\alpha_{L\pm}|^2 = \Phi_{\mathrm{th}}^2 f_\pm^2/(f_{\mathrm{tot}}^2\kappa_{L\pm})$. The input power $P_{\mathrm{in}}^{\pm}$ in each pump mode thus does not depend only on the external driving parameter $\Phi_{\mathrm{in}}^{\pm}$, but also on the driving of the other mode $\Phi_{\mathrm{in}}^{\mp}$. The mode populations as a function of f_+ and f_- are shown in Fig. 2. In particular, it should be noted that there is only a single threshold, below which no stimulated emission occurs, and above which all three output modes are populated. Analysis of the fluctuations around the steady-state values demonstrates that the obtained solutions are stable [33]. Thus, *both* polariton modes show stimulated emission due to the population of the Stokes mode as soon as the total pump power becomes large enough. Consequently, the quantum yield for conversion from each pump mode to the corresponding polariton mode, $\mathcal{Q}_\pm = (P_\pm/\omega_\pm)/(P_{\mathrm{in}}^{\pm}/\omega_{L\pm})$, becomes

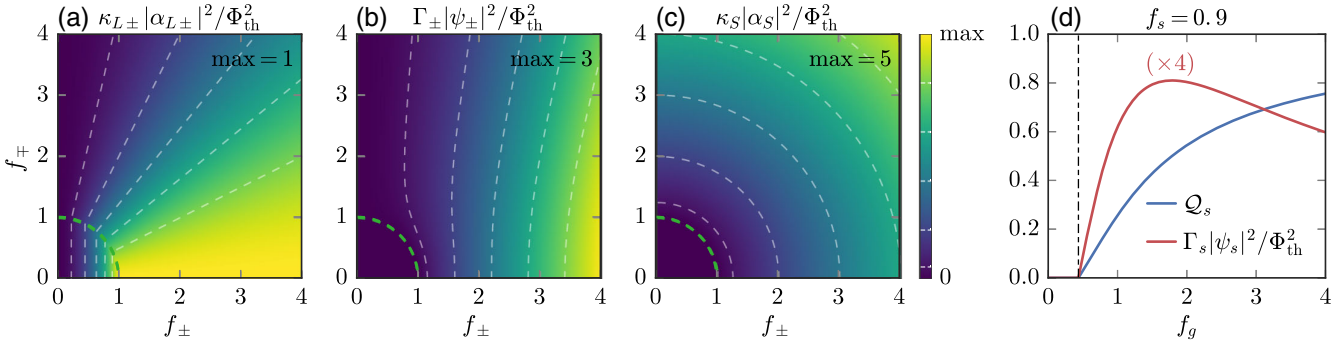

FIG. 2. Rescaled population densities under two-mode pumping with $\Phi_{\rm th}^{+} = \Phi_{\rm th}^{-}$, for (a) the pump mode, (b) the polaritons, and (c) the Stokes mode. The green dashed semicircles denote the threshold condition $f_{\rm tot} \geq 1$. (d) Quantum efficiency $\mathcal{Q}_S$ (blue line) and rescaled signal polariton density (red line, multiplied by 4 for clarity) at a signal pump strength of $f_s = 0.9$ as a function of the gate pump strength f_g.

$$\mathcal{Q}_{+} = \mathcal{Q}_{-} = 1 - \frac{1}{f_{\rm tot}}, \tag{14}$$

where $P_{\rm in}^{\pm} = \omega_{L\pm}\sqrt{\kappa_{L\pm}}\Phi_{\rm in}^{\pm}|\alpha_{L\pm}|$ is the input power in pump mode $L\pm$ [33]. In contrast to the "normal" OPO case in Eq. (8), the quantum yield of a given polariton does not depend on the corresponding input power ($\propto f_{\pm}^2$), but only on the total one ($\propto f_{\rm tot}^2$). This demonstrates that the system can indeed be used like a switch, as sketched above: A below-threshold signal beam input $f_s < 1$ does not produce output in the signal polariton if the gate beam is turned off, but is efficiently converted to signal polaritons if the gate is switched on ($f_g^2 > 1 - f_s^2$). The conversion efficiency of the signal can be made high by making the gate beam sufficiently strong, as demonstrated in Fig. 2(d). The switching speed is limited by the lifetime of the longest-lived state in the system, leading to a trade-off between achieving low thresholds (requiring small losses) and fast switching speeds (requiring large losses).

To conclude, we have demonstrated that by taking advantage of the phenomenon of collective vibrational strong coupling, it is feasible to transform a Raman laser into an OPO. On the one hand, this corresponds to a new type of OPO based on Raman scattering, a nonlinear process that does not normally allow OPO operation. This could enable novel solid-state microcavity devices for applications requiring mutually coherent and/or entangled beams in disparate frequency regions. On the other hand, even if the second mid-IR output beam is not used, our approach could improve existing Raman lasers by lowering the operating threshold and reducing heat generation. Moreover, such a device could be used as an optically driven mid-IR source in integrated photonic systems. Finally, thanks to the existence of two similar vibropolaritons, the proposed device could also operate as an all-optical switch when excited by two properly designed external beams. Our finding is thus an example of the great potential that hybrid light-matter states possess in manipulating light fields and providing novel light sources.

This work has been funded by the European Research Council (ERC-2011-AdG Proposal No. 290981), the European Union Seventh Framework Programme under Grant Agreement No. FP7-PEOPLE-2013-CIG-618229, and the Spanish MINECO under Contract No. MAT2014-53432-C5-5-R and through the "María de Maeztu" program for Units of Excellence in R&D (MDM-2014-0377).

*fj.garcia@uam.es
†johannes.feist@uam.es

[1] A. Shalabney, J. George, J. Hutchison, G. Pupillo, C. Genet, and T. W. Ebbesen, Coherent coupling of molecular resonators with a microcavity mode, Nat. Commun. **6**, 5981 (2015).
[2] J. George, A. Shalabney, J. A. Hutchison, C. Genet, and T. W. Ebbesen, Liquid-phase vibrational strong coupling, J. Phys. Chem. Lett. **6**, 1027 (2015).
[3] J. P. Long and B. S. Simpkins, Coherent coupling between a molecular vibration and Fabry-Perot optical cavity to give hybridized states in the strong coupling limit, ACS Photonics **2**, 130 (2015).
[4] J. del Pino, J. Feist, and F. J. Garcia-Vidal, Quantum theory of collective strong coupling of molecular vibrations with a microcavity mode, New J. Phys. **17**, 053040 (2015).
[5] B. S. Simpkins, K. P. Fears, W. J. Dressick, B. T. Spann, A. D. Dunkelberger, and J. C Owrutsky, Spanning strong to weak normal mode coupling between vibrational and Fabry-Pérot cavity modes through tuning of vibrational absorption strength, ACS Photonics **2**, 1460 (2015).
[6] M. Muallem, A. Palatnik, G. D. Nessim, and Y. R. Tischler, Strong light-matter coupling and hybridization of molecular vibrations in a low-loss infrared microcavity, J. Phys. Chem. Lett. **7**, 2002 (2016).
[7] A. Shalabney, J. George, H. Hiura, J. A. Hutchison, C. Genet, P. Hellwig, and T. W. Ebbesen, Enhanced raman scattering from vibro-polariton hybrid states, Angew. Chem. Int. Ed. **54**, 7971 (2015).
[8] J. del Pino, J. Feist, and F. J. Garcia-Vidal, Signatures of vibrational strong coupling in Raman scattering, J. Phys. Chem. C **119**, 29132 (2015).

[9] A. Strashko and J. Keeling, Raman scattering with strongly coupled vibron-polaritons, Phys. Rev. A **94**, 023843 (2016).
[10] A. Penzkofer, A. Laubereau, and W. Kaiser, High intensity Raman interactions, Prog. Quantum Electron. **6**, 55 (1979).
[11] R. H. Stolen, Raman oscillation in glass optical waveguide, Appl. Phys. Lett. **20**, 62 (1972).
[12] H. M. Pask, The design and operation of solid-state Raman lasers, Prog. Quantum Electron. **27**, 3 (2003).
[13] F. Benabid, J. C. Knight, G. Antonopoulos, and P. St. J. Russell, Stimulated Raman scattering in hydrogen-filled hollow-core photonic crystal fiber, Science **298**, 399 (2002).
[14] O. Boyraz and B. Jalali, Demonstration of a silicon Raman laser, Opt. Express **12**, 5269 (2004).
[15] H. Rong, R. Jones, A. Liu, O. Cohen, D. Hak, A. Fang, and M. Paniccia, A continuous-wave Raman silicon laser, Nature (London) **433**, 725 (2005).
[16] H. Rong, S. Xu, Y.-H. Kuo, V. Sih, O. Cohen, O. Raday, and M. Paniccia, Low-threshold continuous-wave Raman silicon laser, Nat. Photonics **1**, 232 (2007).
[17] T. J. Kippenberg, S. M. Spillane, D. K. Armani, and K. J. Vahala, Ultralow-threshold microcavity Raman laser on a microelectronic chip, Opt. Lett. **29**, 1224 (2004).
[18] J. K. Brasseur, K. S. Repasky, and J. L. Carlsten, Continuous-wave Raman laser in H_2, Opt. Lett. **23**, 367 (1998).
[19] R. W. Boyd, *Nonlinear Optics*, 3rd ed. (Elsevier, New York, 2008).
[20] D. F. Walls, Squeezed states of light, Nature (London) **306**, 141 (1983).
[21] M. D. Reid and P. D. Drummond, Quantum Correlations of Phase in Nondegenerate Parametric Oscillation, Phys. Rev. Lett. **60**, 2731 (1988).
[22] M. Xiao, L. A. Wu, and H. J. Kimble, Precision Measurement Beyond the Shot-Noise Limit, Phys. Rev. Lett. **59**, 278 (1987).
[23] A. Heidmann, R. J. Horowicz, S. Reynaud, E. Giacobino, C. Fabre, and G. Camy, Observation of Quantum Noise Reduction on Twin Laser Beams, Phys. Rev. Lett. **59**, 2555 (1987).
[24] S. Ramelow, L. Ratschbacher, A. Fedrizzi, N. K. Langford, and A. Zeilinger, Discrete Tunable Color Entanglement, Phys. Rev. Lett. **103**, 253601 (2009).
[25] A. S. Coelho, F. A. S. Barbosa, K. N. Cassemiro, A. S. Villar, M. Martinelli, and P. Nussenzveig, Three-color entanglement, Science **326**, 823 (2009).
[26] E. Saglamyurek, N. Sinclair, J. Jin, J. A. Slater, D. Oblak, F. Bussières, M. George, R. Ricken, W. Sohler, and W. Tittel, Broadband waveguide quantum memory for entangled photons, Nature (London) **469**, 512 (2011).
[27] A. Lenhard, M. Bock, C. Becher, S. Kucera, J. Brito, P. Eich, P. Müller, and J. Eschner, Telecom-heralded single-photon absorption by a single atom, Phys. Rev. A **92**, 063827 (2015).
[28] H. M. Gibbs, *Optical Bistability: Controlling Light with Light*, Quantum Electronics Series (Academic Press, New York, 1985).
[29] A. M. C. Dawes, L. Illing, S. M. Clark, and D. J. Gauthier, All-optical switching in rubidium vapor, Science **308**, 672 (2005).
[30] H. J. Carmichael, *Statistical Methods in Quantum Optics 2: Non-Classical Fields*, Theoretical and Mathematical Physics (Springer, Berlin, 2008), p. 542.
[31] E. Brion, L. H. Pedersen, and K. Mølmer, Adiabatic elimination in a lambda system, J. Phys. A **40**, 1033 (2007).
[32] F. Reiter and A. S. Sørensen, Effective operator formalism for open quantum systems, Phys. Rev. A **85**, 032111 (2012).
[33] See Supplemental Material at http://link.aps.org/supplemental/10.1103/PhysRevLett.117.277401, which includes Refs. [34–37], for details on the adiabatic elimination of the electronically excited states, a possible distributed Bragg reflector-based implementation of the proposed setup, the general solution under double pumping, and the stability analysis.
[34] H. Feshbach, Unified theory of nuclear reactions, Ann. Phys. (N.Y.) **5**, 357 (1958).
[35] *Handbook of Optical Constants*, edited by E. D. Palik (Academic Press, New York, 1991), Vol. 2.
[36] K. S. Daskalakis, S. A. Maier, R. Murray, and S. Kéna-Cohen, Nonlinear interactions in an organic polariton condensate, Nat. Mater. **13**, 271 (2014).
[37] I. Solomonovich Gradshteyn and I. Moiseevich Ryzhik, *Table of Integrals, Series, and Products*, 8th ed., edited by D. Zwillinger (Elsevier, New York, 2014).
[38] S. Kéna-Cohen and S. R. Forrest, Room-temperature polariton lasing in an organic single-crystal microcavity, Nat. Photonics **4**, 371 (2010).
[39] R. Houdré, R. P. Stanley, and M. Ilegems, Vacuum-field Rabi splitting in the presence of inhomogeneous broadening: Resolution of a homogeneous linewidth in an inhomogeneously broadened system, Phys. Rev. A **53**, 2711 (1996).
[40] H.-P. Breuer and F. Petruccione, *The Theory of Open Quantum Systems* (Oxford University Press, New York, 2007), p. 636.
[41] A. Yariv and W. H. Louisell, 5A2—Theory of the optical parametric oscillator, IEEE J. Quantum Electron. **2**, 418 (1966).
[42] J. Kasprzak, M. Richard, S. Kundermann, A. Baas, P. Jeambrun, J. M. J. Keeling, F. M. Marchetti, M. H. Szymańska, R. André, J. L. Staehli, V. Savona, P. B. Littlewood, B. Deveaud, and Le Si Dang, Bose-Einstein condensation of exciton polaritons, Nature (London) **443**, 409 (2006).